Multirate Feedforward Control based on Modal Form with Mode Selection Applied to Multi-Modal High-Precision Positioning Stage

Masahiro Mae, Wataru Ohnishi and Hiroshi Fujimoto
The University of Tokyo
5-1-5, Kashiwanoha, Kashiwa, Chiba, 277-8561, Japan
Phone: +81-4-7136-3881
Email: mmae@ieee.org, ohnishi@ieee.org, fujimoto@k.u-tokyo.ac.jp

***Abstract*—Multirate feedforward control provides perfect tracking control for the desired state trajectory in the model. The aim of this paper is the analysis of multirate feedforward control based on modal form with mode selection. The proposed approach is applied for a mechanical system that has several modes and a multirate feedforward controller is designed depending on the mode selection. The approach is successfully applied to an 8th order motion system. The proposed approach improves the intersample behavior of tracking error compared with multirate feedforward control based on controllable canonical form.**

***Index Terms*—multirate feedforward control, modal form, perfect tracking control, intersample behavior**

I. Introduction

Inverse model feedforward control plays an important role in tracking control problems in high-precision mechatronic systems, such as wafer and LCD scanners [1], [2], atomic force microscopes [3], and hard disc drives [4]. If the model has unstable zeros, the feedforward controller has unstable poles because it is designed as the inverse of the model. The feedforward controller with unstable poles generates an unbounded control input and it is not applicable for the real motion systems. When the model does not have unstable intrinsic zeros in continuous-time, the discretized model has unstable discretization zeros when the relative degree of the model is two or more such as many rigid systems in mechatronic systems [5]. The inverse model feedforward controller designed for the model with unstable discretization zeros has unstable poles and unbounded or oscillating control inputs are generated.

To overcome the unstable zero problems of the model, several approximate inversion approaches are developed, such as zero phase error tracking control (ZPETC) [6], zero magnitude error tracking control (ZMETC) [7], and nonminimum-phase zeros ignore (NPZ-Ignore) [8]. However, these approaches are using approximate inversion of the model and perfect tracking control defined in [6] cannot be achieved, theoretically.

Multirate feedforward control [9] is proposed to solve unstable discretization zero problems and to achieve perfect tracking control. The multirate feedforward control provides an exact state tracking at every n samples for nth order model. The discrete-time stable inversion approach [10], [11] is also proposed, however, this approach treats the unstable intrinsic and discretization zeros in the same way, and preactuated control inputs are generated for not only the unstable intrinsic zeros but also unstable discretization zeros. On the other hand, the multirate feedforward control approach designed the independent stable inversion of unstable intrinsic and discretization zeros [12]. Therefore, the advantage is that the multirate feedforward controller does not generate preactuated feedforward control inputs for unstable discretization zeros.

A higher-order accurate model improves the tracking performance of inverse model feedforward controllers. However, the multirate feedforward control has the trade-off between the number of states which achieve perfect tracking and the sampling intervals when the perfect tracking is achieved. For the nth-order model with the sampling period of control input T_u, the exact state tracking is achieved every nT_u and it is the same case with a minimum-time dead-beat control [13]. This problem is also known that the higher-order model is numerically ill-conditioned in designing inverse model feedforward controllers.

Multirate feedforward control based on the modal form [14] is proposed to improve these problems because of higher-order models. Previous research shows that multirate feedforward control based on the modal form achieves the exact state tracking for selected modes in shorter intervals and improves continuous-time tracking error. The condition number is also improved compared with conventional multirate feedforward control. In this approach, there is a degree of freedom to select which modes for state tracking. The aim of this paper is to clarify the relationship between mode selection and continuous-time tracking error in multirate feedforward control based on modal form.

The outline of this paper is as follows. In Section II, the control objective is formulated. Desired state trajectory generation method for multirate feedforward control is presented in Section III. Multirate feedforward control based on modal form is presented in Section IV. The advantages of the approach are demonstrated in Section V. Conclusions are presented in Section VI.

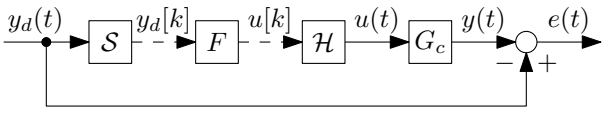

Fig. 1. Block diagram of tracking control. The continuous-time system G_c is controlled by the discrete-time controller F with sampler $\mathcal{S}$ and holder $\mathcal{H}$. The objective is to minimize the continuous-time error $e(t)$.

II. Problem formulation

In this section, the control problem is formulated. The overview of the control problem is shown in Fig. 1, with desired output trajectory $y_d(t) \in \mathbb{R}$, control input $u(t) \in \mathbb{R}$, output $y(t) \in \mathbb{R}$, digital controller F, sampler $\mathcal{S}$, and zero-order hold $\mathcal{H}$. The continuous-time linear-time-invariant (LTI) nth-order system G_c is given by

$$G_c(s) = \frac{B(s)}{A(s)} = \frac{b_m s^m + \cdots + b_1 s + b_0}{s^n + a_{n-1}s^{n-1} + \cdots + a_1 s + a_0}, \quad (1)$$

where $m, n \in \mathbb{N}$, $n > m$, and $b_0 \neq 0$. It is assumed that G_c is minimal realization, stable, and with no unstable intrinsic zero.

The control objective of this paper is minimizing the continuous-time error e. The desired output trajectory y_d is assumed to be known a priori. The preactuated control input which is used in negative time is not used in this control problem.

III. State trajectory generation based on controllable canonical form

In this section, the state trajectory generation method based on controllable canonical form is presented. Multirate feedforward control achieves perfect tracking control for the desired state trajectory $\boldsymbol{x}_d$ at every reference sampling period. The desired state trajectory $\boldsymbol{x}_d$ is generated from the desired output trajectory y_d with the system of controllable canonical form.

The controllable canonical form of (1) is given by

$$\dot{\boldsymbol{x}}_{ccf}(t) = \boldsymbol{A}_{c,ccf}\boldsymbol{x}_{ccf}(t) + \boldsymbol{b}_{c,ccf}u(t), \quad (2)$$
$$y(t) = \boldsymbol{c}_{c,ccf}\boldsymbol{x}_{ccf}(t), \quad (3)$$

where

$$\boldsymbol{x}_{ccf}(t) = \begin{bmatrix} x_{0,ccf}(t) & x_{1,ccf}(t) & \cdots & x_{n-1,ccf}(t) \end{bmatrix}^\mathsf{T}, \quad (4)$$

$$\left[\begin{array}{c|c} \boldsymbol{A}_{c,ccf} & \boldsymbol{b}_{c,ccf} \\ \hline \boldsymbol{c}_{c,ccf} & 0 \end{array}\right] = \left[\begin{array}{ccccc|c} 0 & 1 & 0 & \cdots & 0 & 0 \\ 0 & 0 & 1 & \cdots & 0 & 0 \\ \vdots & \vdots & \vdots & \ddots & \vdots & \vdots \\ 0 & 0 & 0 & \cdots & 1 & 0 \\ -a_0 & -a_1 & -a_2 & \cdots & -a_{n-1} & b_0 \\ \hline 1 & \frac{b_1}{b_0} & \frac{b_2}{b_0} & \cdots & 0 & 0 \end{array}\right]. \quad (5)$$

It is assumed that the desired output trajectory $y_d(t)$ is $n-1$ times differentiable, and

$$\boldsymbol{y}_d(t) = \begin{bmatrix} 1 & \frac{\mathrm{d}}{\mathrm{d}t} & \cdots & \frac{\mathrm{d}^{n-1}}{\mathrm{d}t^{n-1}} \end{bmatrix}^\mathsf{T} y_d(t). \quad (6)$$

The desired state trajectory $\boldsymbol{x}_d(t)$ is given by

$$\boldsymbol{x}_{d,ccf}(t) = \mathcal{L}^{-1}\left[\frac{1}{B(s)}\boldsymbol{y}_d(s)\right], \quad (7)$$

where $\mathcal{L}^{-1}(\cdot)$ is the inverse uni-lateral Laplace transform [15].

IV. Multirate feedforward control based on modal form

In this section, the design procedure of the multirate feedforward control based on modal form is presented.

A. Transformation to modal form

The system G_c in (1) is decomposed into second-order modes as follows:

$$G_c(s) = \sum_{l=1}^{n_{mod}} \frac{b_{1,l}s + b_{0,l}}{s^2 + a_{1,l}s + a_{0,l}}, \quad (8)$$

where $n_{mod} \in \mathbb{N}$ is the number of modes and $l \in \mathbb{N}$ is the index of the modes. It is assumed that the system G_c is a mechanical system and consists of a second-order rigid mode and second-order vibration modes. From these assumptions, n is even and $n_{mod} = n/2$.

The state space realization of (8) in which each mode is second-order controllable canonical form is given by

$$\dot{\boldsymbol{x}}_{mod}(t) = \boldsymbol{A}_{c,mod}\boldsymbol{x}_{mod}(t) + \boldsymbol{b}_{c,mod}u(t), \quad (9)$$
$$y(t) = \boldsymbol{c}_{c,mod}\boldsymbol{x}_{mod}(t), \quad (10)$$

where

$$\boldsymbol{x}_{mod}(t) = \begin{bmatrix} \boldsymbol{x}_{mod,1}(t) & \boldsymbol{x}_{mod,2}(t) & \cdots & \boldsymbol{x}_{mod,n_{mod}}(t) \end{bmatrix}^\mathsf{T}, \quad (11)$$

$$\boldsymbol{x}_{mod,l}(t) = \begin{bmatrix} x_{0,mod,l}(t) & x_{1,mod,l}(t) \end{bmatrix}^\mathsf{T} \quad (l = 1, \ldots, n_{mod}), \quad (12)$$

$$\left[\begin{array}{c|c} \boldsymbol{A}_{c,mod} & \boldsymbol{b}_{c,mod} \\ \hline \boldsymbol{c}_{c,mod} & 0 \end{array}\right] = \left[\begin{array}{ccc|c} \boldsymbol{A}_{c,mod,1} & & \boldsymbol{O} & \boldsymbol{b}_{c,mod,1} \\ & \boldsymbol{A}_{c,mod,2} & & \boldsymbol{b}_{c,mod,2} \\ & & \ddots & \vdots \\ \boldsymbol{O} & & \boldsymbol{A}_{c,mod,n_{mod}} & \boldsymbol{b}_{c,mod,n_{mod}} \\ \hline \boldsymbol{c}_{c,mod,1} & \boldsymbol{c}_{c,mod,2} & \cdots \; \boldsymbol{c}_{c,mod,n_{mod}} & 0 \end{array}\right], \quad (13)$$

$$\left[\begin{array}{c|c} \boldsymbol{A}_{c,mod,l} & \boldsymbol{b}_{c,mod,l} \\ \hline \boldsymbol{c}_{c,mod,l} & 0 \end{array}\right] = \left[\begin{array}{cc|c} 0 & 1 & 0 \\ -a_{0,l} & -a_{1,l} & b_{0,l} \\ \hline 1 & \frac{b_{1,l}}{b_{0,l}} & 0 \end{array}\right]. \quad (14)$$

The transformation matrix from controllable canonical form is given by

$$\boldsymbol{T} = \begin{bmatrix} \boldsymbol{b}_{c,mod} & \boldsymbol{A}_{c,mod}\boldsymbol{b}_{c,mod} & \cdots & \boldsymbol{A}_{c,mod}^{(n_{mod}-1)}\boldsymbol{b}_{c,mod} \end{bmatrix} \begin{bmatrix} \frac{a_1}{b_0} & \cdots & \frac{a_{n-1}}{b_0} & \frac{1}{b_0} \\ \vdots & \iddots & \iddots & \\ \frac{a_{n-1}}{b_0} & \frac{1}{b_0} & & \\ \frac{1}{b_0} & & & \boldsymbol{O} \end{bmatrix}. \quad (15)$$

The desired state trajectory in modal form is given by

$$\boldsymbol{x}_{d,mod}(t) = \boldsymbol{T}\boldsymbol{x}_{d,ccf}(t). \quad (16)$$

B. Mode selection

The state space realization (13) is decoupled between the modes. Therefore, the feedforward control input can be generated for selected modes.

The mode selection matrix $\boldsymbol{M}_\mu$ is defined as

$$\boldsymbol{M}_\mu = \mathrm{diag}\{\boldsymbol{M}_l\} \quad (l = 1, \ldots, n_{mod}), \tag{17}$$

$$\boldsymbol{M}_l = \begin{cases} \boldsymbol{I}_{(2,2)} & \text{(selected mode)} \\ \boldsymbol{O}_{(2,2)} & \text{(not selected mode)} \end{cases}, \tag{18}$$

where μ is the indicies of selected modes. The rows of $\boldsymbol{M}$ whose all elements are zeros are eliminated, and

$$\nu = \mathrm{number}\{\mu\}. \tag{19}$$

where $\nu \in \mathbb{N}$ is the number of selected modes μ and $\boldsymbol{M} \in \mathbb{R}^{2\nu \times n}$ (e.g. $\mu = (1, 2)$ then $\nu = 2$).

The state equation with selected modes in (9) is given by

$$\dot{\boldsymbol{x}}_\mu(t) = \boldsymbol{A}_{c,\mu}\boldsymbol{x}_\mu(t) + \boldsymbol{b}_{c,\mu}u(t), \tag{20}$$

where

$$\boldsymbol{x}_\mu(t) = \boldsymbol{M}_\mu\boldsymbol{x}_{mod}(t), \tag{21}$$

$$\boldsymbol{A}_{c,\mu} = \boldsymbol{M}_\mu\boldsymbol{A}_{c,mod}, \tag{22}$$

$$\boldsymbol{b}_{c,\mu} = \boldsymbol{M}_\mu\boldsymbol{b}_{c,mod}. \tag{23}$$

The desired state trajectory with selected modes is also given by

$$\boldsymbol{x}_{d,\mu}(t) = \boldsymbol{M}_\mu\boldsymbol{x}_{d,mod}(t). \tag{24}$$

C. Feedforward control input generation

The feedforward control input is generated with selected modes. The discretized system of (20) with a sampling period of control input T_u is given by

$$\boldsymbol{x}_\mu[k+1] = \boldsymbol{A}_{s,\mu}\boldsymbol{x}_\mu[k] + \boldsymbol{b}_{s,\mu}u[k], \tag{25}$$

where

$$\boldsymbol{A}_{s,\mu} = e^{\boldsymbol{A}_{c,\mu}T_u}, \quad \boldsymbol{b}_{s,\mu} = \int_0^{T_u} e^{\boldsymbol{A}_{c,\mu}\tau}\boldsymbol{b}_{c,\mu}\mathrm{d}\tau. \tag{26}$$

The state equation of the lifted system with input multiplicity 2ν is given by

$$\boldsymbol{x}_\mu[i+1] = \boldsymbol{A}_\mu\boldsymbol{x}_\mu[i] + \boldsymbol{B}_\mu\boldsymbol{u}[i], \tag{27}$$

where a sampling period of reference $T_r = 2\nu T_u$ and

$$\boldsymbol{x}_\mu[i] = \boldsymbol{x}_\mu(iT_r), \tag{28}$$

$$\boldsymbol{A}_\mu = \boldsymbol{A}_{s,\mu}^{2\nu}, \tag{29}$$

$$\boldsymbol{B}_\mu = \begin{bmatrix} \boldsymbol{A}_{s,\mu}^{2\nu-1}\boldsymbol{b}_{s,\mu} & \boldsymbol{A}_{s,\mu}^{2\nu-2}\boldsymbol{b}_{s,\mu} & \cdots & \boldsymbol{b}_{s,\mu} \end{bmatrix}, \tag{30}$$

$$\begin{aligned} \boldsymbol{u}[i] &= \begin{bmatrix} u_1 & u_2 & \cdots & u_{2\nu} \end{bmatrix} \\ &= \begin{bmatrix} u(kT_u) & u((k+1)T_u) & \cdots & u((k+2\nu-1)T_u) \end{bmatrix}. \end{aligned} \tag{31}$$

From (27), the feedforward control input $\boldsymbol{u}_{ff}[i]$ is generated with 2ν sample previewed desired state trajectory $\boldsymbol{x}_{d,\mu}[i+1]$ as follows:

$$\boldsymbol{u}_{ff}[i] = \boldsymbol{B}_\mu^{-1}(\boldsymbol{I} - z^{-1}\boldsymbol{A}_\mu)\boldsymbol{x}_{d,\mu}[i+1], \tag{32}$$

where $z = e^{s2\nu T_u}$.

The overview of the proposed approach is shown in Fig. 2. The feedforward control input $\boldsymbol{u}_{ff}$ realizes the perfect state tracking in every $T_r = 2\nu T_u$ for selected modes. Note that this approach does not guarantee the perfect state tracking for other modes, but, they also reasonably tracking. It is because the desired state trajectory is generated considering other modes in (16).

Compared to the multirate feedforward control based on controllable canonical form that archives the perfect state tracking for all modes in every $T_r = nT_u$, the proposed approach achieves the perfect state tracking for selected modes in a shorter period. The shorter tracking period improves the intersample behavior and leads to reduce continuous-time tracking error.

It is also the advantage of the proposed approach that the order of the matrix $\boldsymbol{B}_\mu$ in (32) is reduced because of mode selection. The matrix $\boldsymbol{B}_\mu$ is the same as the controllability matrix and is numerically ill-conditioned in higher-order systems. The previous research shows that the proposed approach outperforms the conventional multirate feedforward for the model with simple mode reduction [14].

In the proposed approach, the problem of the unstable intrinsic and discretization zeros is treated in the state trajectory generation and multirate feedforward control, separately [12]. Therefore, when the system does not have intrinsic zeros, the advantage of the proposed approach is that it does not use preactuation because of the unstable discretization zeros.

V. Simulation

In this section, the proposed approach is applied to a motion system. The results demonstrate the advantage of the proposed approach.

A. Setup

The motion system of a high-precision positioning stage is illustrated in Fig. 3(a). The continuous-time transfer function from the input current u [A] generating the force with the linear motor to the output displacement y [m] measured by the linear encoder is given by

$$\begin{aligned} G_c(s) = &\frac{4.5759 \times 10^6(s^2 + 8.132s + 2.518 \times 10^4)}{s(s + 2.101)(s^2 + 10.89s + 3.665 \times 10^4)} \\ &\times \frac{(s^2 + 84.73s + 8.497 \times 10^5)}{(s^2 + 45.4s + 3.139 \times 10^5)(s^2 + 262.2s + 3.507 \times 10^6)} \end{aligned} \tag{33}$$

and is minimal realization, stable, and with no unstable intrinsic zero. The Bode diagram of the motion system G_c is shown in Fig. 3(b).

G_c is decomposed to four second-order modes as follows:

$$\begin{aligned} G_c(s) &= G_{1c}(s) + G_{2c}(s) + G_{3c}(s) + G_{4c}(s) \\ &= \frac{-0.00027976(s - 8674)}{s(s + 2.101)} + \frac{-0.00012742(s - 9494)}{(s^2 + 10.89s + 3.665 \times 10^4)} \\ &\quad + \frac{0.00032577(s - 7779)}{(s^2 + 45.4s + 3.139 \times 10^5)} + \frac{8.1406 \times 10^{-5}(s - 1.312 \times 10^4)}{(s^2 + 262.2s + 3.507 \times 10^6)}. \end{aligned} \tag{34}$$

The Bode diagrams of four second-order modes from G_{1c} to G_{4c} are shown in Fig. 3(c).

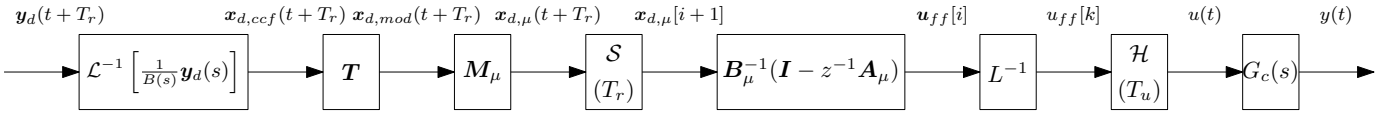

Fig. 2. Block diagram of state trajectory generation and multirate feedforward control based on modal form. z, $\mathcal{S}$, $\mathcal{H}$, and L denote e^{sT_r}, sampler, holder, and lifting operator [16], respectively.

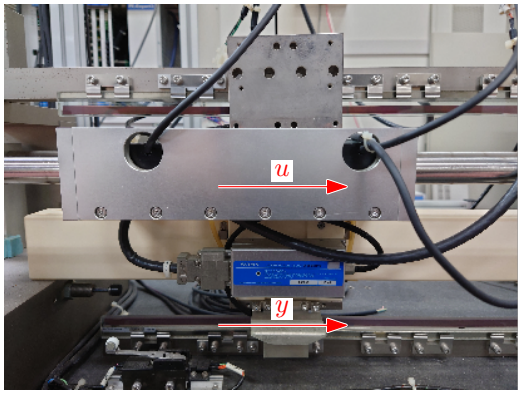

(a) High-precision positioning stage with input current u [A] generating force with linear motor and output displacement y [m] measured by linear encoder.

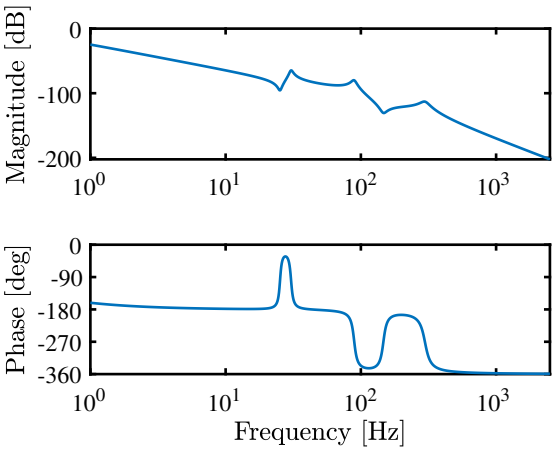

(b) Bode diagram of 8th-order motion system: $G_c(s)$ (——).

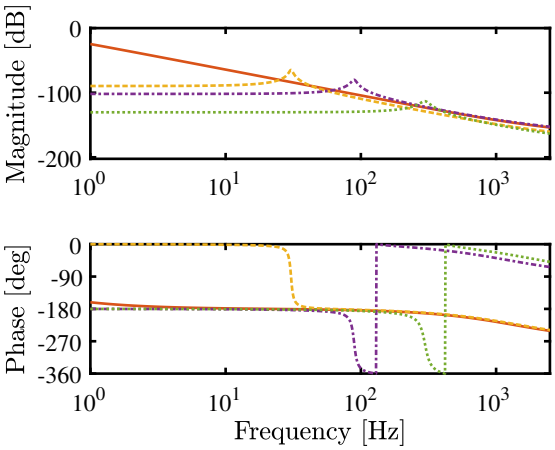

(c) Bode diagram of four second-order modes: $G_{1c}(s)$ (——), $G_{2c}(s)$ (– – –), $G_{3c}(s)$ (–·–·–), and $G_{4c}(s)$ (·····).

Fig. 3. High-precision positioning stage used in simulations.

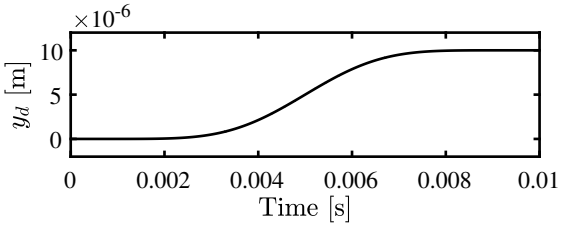

Fig. 4. Desired output trajectory y_d consists of 15th-order polynomials.

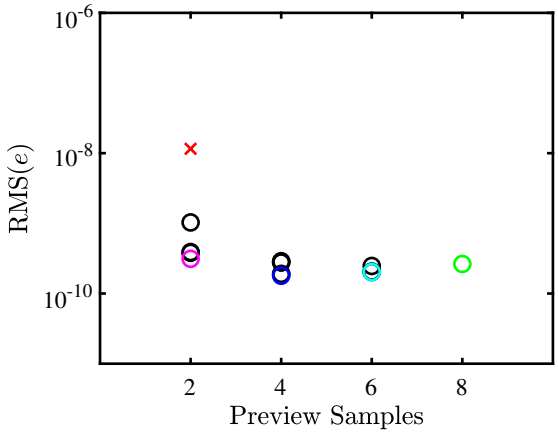

(a) RMS(e)

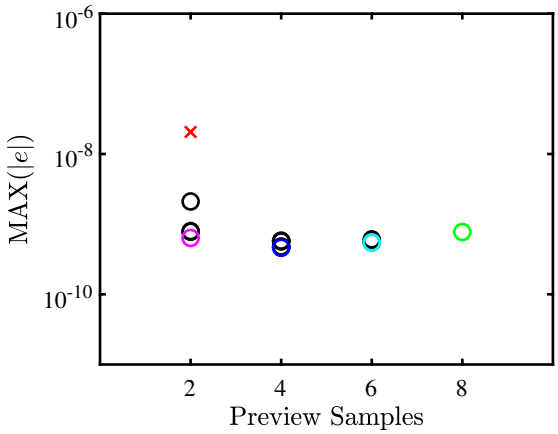

(b) MAX($|e|$)

Fig. 5. Preview samples versus root mean square errors RMS(e) and maximum absolute errors MAX($|e|$) of simulations depending on mode selection μ. ○ shows the errors of multirate feedforward control based on modal form, e.g., ○: $\mu = (3)$, ○: $\mu = (3,4)$, ○: $\mu = (2,3,4)$, and ○: $\mu = (1,2,3,4)$. × shows the errors of conventional ZPETC.

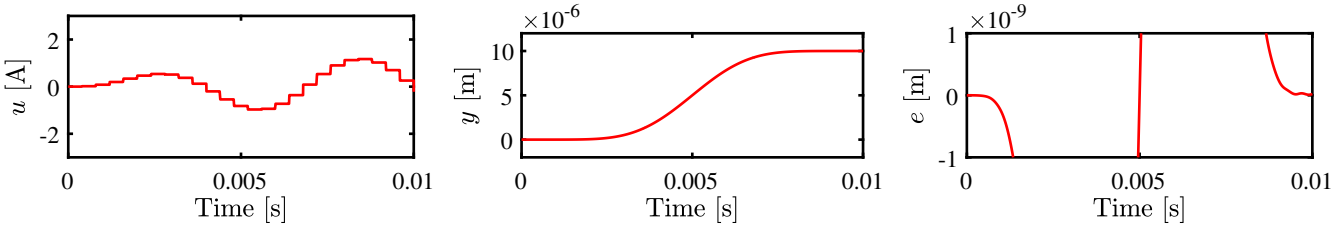

(a) Input u (b) Output y (c) Error e

Fig. 6. Simulation results of input u, output y, and error e using conventional ZPETC (——).

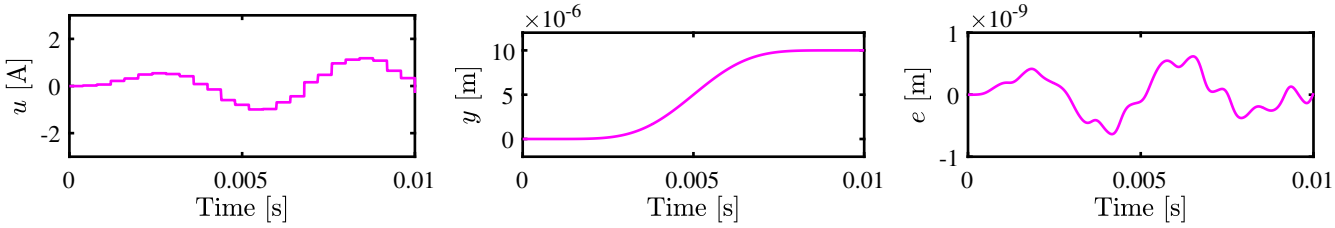

(a) Input u (b) Output y (c) Error e

Fig. 7. Simulation results of input u, output y, and error e using multirate feedforward control with mode selection $\mu = (3)$ (——).

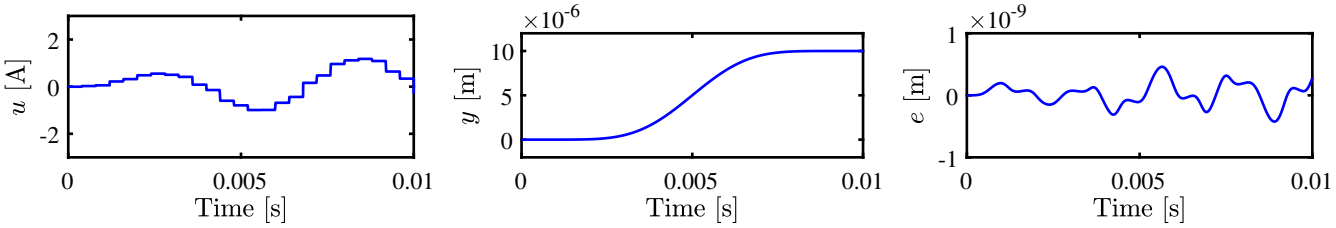

(a) Input u (b) Output y (c) Error e

Fig. 8. Simulation results of input u, output y, and error e using multirate feedforward control with mode selection $\mu = (3, 4)$ (——).

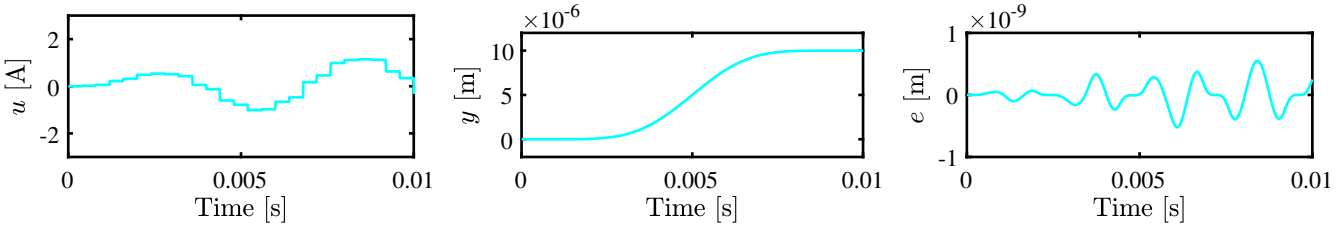

(a) Input u (b) Output y (c) Error e

Fig. 9. Simulation results of input u, output y, and error e using multirate feedforward control with mode selection $\mu = (2, 3, 4)$ (——).

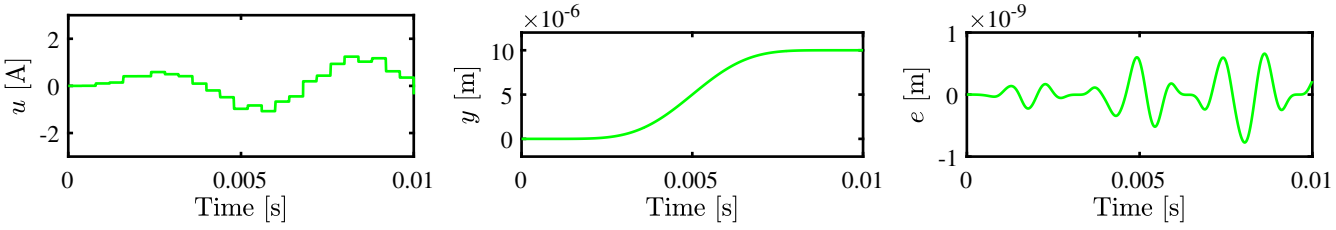

(a) Input u (b) Output y (c) Error e

Fig. 10. Simulation results of input u, output y, and error e using multirate feedforward control with mode selection $\mu = (1, 2, 3, 4)$ (——).

TABLE I
ROOT MEAN SQUARE ERRORS $\mathrm{RMS}(e)$ AND MAXIMUM ABSOLUTE ERRORS $\mathrm{MAX}(|e|)$ OF SIMULATIONS DEPENDING ON MODE SELECTION μ.

μ	$\mathrm{RMS}(e)$ [m]	$\mathrm{MAX}(\lvert e\rvert)$ [m]
ZPETC	1.16×10^{-08}	2.06×10^{-08}
(1)	3.90×10^{-10}	7.96×10^{-10}
(2)	3.80×10^{-10}	7.80×10^{-10}
(3)	3.12×10^{-10}	6.36×10^{-10}
(4)	1.03×10^{-09}	2.11×10^{-09}
$(1,2)$	2.89×10^{-10}	5.81×10^{-10}
$(1,3)$	2.79×10^{-10}	5.73×10^{-10}
$(1,4)$	1.90×10^{-10}	4.79×10^{-10}
$(2,3)$	2.78×10^{-10}	5.71×10^{-10}
$(2,4)$	1.89×10^{-10}	4.72×10^{-10}
$(3,4)$	1.79×10^{-10}	4.60×10^{-10}
$(1,2,3)$	2.47×10^{-10}	6.07×10^{-10}
$(1,2,4)$	2.05×10^{-10}	5.64×10^{-10}
$(1,3,4)$	2.02×10^{-10}	5.51×10^{-10}
$(2,3,4)$	2.02×10^{-10}	5.50×10^{-10}
$(1,2,3,4)$	2.64×10^{-10}	7.73×10^{-10}

B. Conditions

The reference of the desired output trajectory y_d is given by a 15th-order polynomial which change from 0 to $10\,\mu\mathrm{m}$ in $0\,\mathrm{s}$ to $10\,\mathrm{ms}$ as shown in Fig. 4. The sampling period of the control input is set to $T_u = 400\,\mu\mathrm{s}$.

In this simulation, the indicies of selected modes μ is defined as follows:

$$\mu = (1),(2),(3),(4),(1,2),(1,3),(1,4),(2,3),(2,4),(3,4),\\ (1,2,3),(1,2,4),(1,3,4),(2,3,4),(1,2,3,4). \quad (35)$$

Note that the case with $\mu = (1,2,3,4)$ selected all modes and it is the same to the conventional multirate feedforward control based on controllable canonical form. The proposed approach is compared with the ZPETC [6] as the conventional method. The system is controlled in open loop.

C. Results

The root mean square errors $\mathrm{RMS}(e)$ and the maximum absolute errors $\mathrm{MAX}(|e|)$ of simulations in all cases with the numbers of preview samples are illustrated in Fig. 5. The root mean square errors $\mathrm{RMS}(e)$ and the maximum absolute errors $\mathrm{MAX}(|e|)$ are shown in TABLE I. From these results, all cases of the proposed approach outperform the conventional ZPETC, and the mode selection $\mu = (3,4)$ is the best tracking performance for the desired output trajectory.

The mode selections $\mu = (3),(3,4),(2,3,4),(1,2,3,4)$ that are the best control performance in each preview samples are compared with the conventional ZPETC. The simulation results are shown from Fig. 6 to Fig. 10. From these results, the proposed approaches outperform the conventional ZPETC. It is also confirmed that the proposed approaches with mode selections, $\mu = (3),(3,4),(2,3,4)$, do not achieve perfect on-sample tracking to the desired output trajectory compared with the conventional multirate feedforward control, $\mu = (1,2,3,4)$, theoretically. However, the approaches with $\mu = (3,4),(2,3,4)$ achieve better tracking performance in the objective of the continuous-time error reduction.

The results demonstrate the advantage of the proposed approach in the objective of minimizing the continuous-time error.

VI. CONCLUSION

Multirate feedforward control based on modal form with mode selection is developed. The proposed approach improves the intersample behavior of tracking error compared with multirate feedforward control based on controllable canonical form. The advantages of the approach are validated in the simulations of the 8th-order motion system. Ongoing research focuses on the relationship between the reference trajectory and the mode selection in multirate feedforward control based on modal form.

REFERENCES

[1] T. Oomen, "Advanced Motion Control for Precision Mechatronics: Control, Identification, and Learning of Complex Systems," *IEEJ Journal of Industry Applications*, vol. 7, no. 2, pp. 127–140, 2018.

[2] M. Mae, W. Ohnishi, H. Fujimoto, and Y. Hori, "Perfect Tracking Control Considering Generalized Controllability Indices and Application for High-Precision Stage in Translation and Pitching," *IEEJ Journal of Industry Applications*, vol. 8, no. 2, pp. 263–270, mar 2019.

[3] S. Ito, S. Troppmair, F. Cigarini, and G. Schitter, "High-speed Scanner with Nanometer Resolution Using a Hybrid Reluctance Force Actuator," *IEEJ Journal of Industry Applications*, vol. 8, no. 2, pp. 170–176, mar 2019.

[4] S. Nakagawa, T. Yamaguchi, I. Fujimoto, Y. Hori, Y. Ito, and Y. Hata, "Multi-rate two-degree-of-freedom control for fast and vibration-less seeking of hard disk drives," in *Proceedings of the 2001 American Control Conference*, vol. 4. IEEE, 2001, pp. 2797–2802 vol.4.

[5] K. Åström, P. Hagander, and J. Sternby, "Zeros of sampled systems," *Automatica*, vol. 20, no. 1, pp. 31–38, jan 1984.

[6] M. Tomizuka, "Zero Phase Error Tracking Algorithm for Digital Control," *Journal of Dynamic Systems, Measurement, and Control*, vol. 109, no. 1, p. 65, 1987.

[7] J. Wen and B. Potsaid, "An experimental study of a high performance motion control system," in *Proceedings of the 2004 American Control Conference*, vol. 6. IEEE, 2004, pp. 5158–5163.

[8] J. Butterworth, L. Pao, and D. Abramovitch, "Analysis and comparison of three discrete-time feedforward model-inverse control techniques for nonminimum-phase systems," *Mechatronics*, vol. 22, no. 5, pp. 577–587, aug 2012.

[9] H. Fujimoto, Y. Hori, and A. Kawamura, "Perfect tracking control based on multirate feedforward control with generalized sampling periods," *IEEE Transactions on Industrial Electronics*, vol. 48, no. 3, pp. 636–644, jun 2001.

[10] J. van Zundert and T. Oomen, "On inversion-based approaches for feedforward and ILC," *Mechatronics*, vol. 50, no. November 2016, pp. 282–291, 2018.

[11] J. Van Zundert, W. Ohnishi, H. Fujimoto, and T. Oomen, "Improving Intersample Behavior in Discrete-Time System Inversion: With Application to LTI and LPTV Systems," *IEEE/ASME Transactions on Mechatronics*, vol. PP, no. c, pp. 1–1, 2019.

[12] W. Ohnishi, T. Beauduin, and H. Fujimoto, "Preactuated Multirate Feedforward Control for Independent Stable Inversion of Unstable Intrinsic and Discretization Zeros," *IEEE/ASME Transactions on Mechatronics*, vol. 24, no. 2, pp. 863–871, apr 2019.

[13] G. C. Goodwin, S. F. Graebe, and M. E. Salgado, *Control System Design*, 2000.

[14] W. Ohnishi and H. Fujimoto, "Multirate Feedforward Control Based on Modal Form," in *2018 IEEE Conference on Control Technology and Applications (CCTA)*, no. 2. IEEE, aug 2018, pp. 1120–1125.

[15] A. V. Oppenheim, A. S. Willsky, and S. Nawab, *Signals and Systems*, 2nd ed. Prentice-Hall, Inc., 1997.

[16] T. Chen and B. A. Francis, *Optimal Sampled-Data Control Systems*. London: Springer London, 1995.